Article

a special issue for the scientific conference held by the Department of Chemistry- College of Education for Girls/University of Kufa,under the title:
(6'th Postgraduate Students Annual Conference) (PSAC2025).
which held for Tuesday, 15/4/2025.

Experimental study of the adsorption of eosin yellow dye on the surface of coal derived from walnut shells and a theoretical study through density functional theory

Estabrqa Arif Mohammed[1], Lekaa Hussain Khadim[2]
*Department of chemistry, College of education for women, University of Kufa, Al Najaf Al-Ashraf, Iraq
[1]estabrqa.aljanabi@student.uokufa.edu.iq, [2]liqaa.aljailawi@uokufa.edu.iq

Abstract

Since water pollution constitutes a large part of the pollutants spread on the surface of the earth, pollution is unfortunately the most deadly silent weapon in the world today, especially in light of technological progress. Many efforts have been made to get rid of these pollutants. This study aimed to purify water from pollutants and determine the ideal conditions to improve the adsorption process of eosin yellow dye on the surface of activated carbon derived from walnut shells. Several studies have found that different acidity functions, contact times (512 min for dye), and temperatures (ranging from 298 to 328 K) all played an important role. The adsorption curves were also studied as they apply to Temkin and studying the kinetics of the reaction, and the second-order reaction was reached through the R^2 value, which was the highest theoretical value by studying the dye in the optimized geometries in the basic case B3LYP and the basis sets 6-311G using density functional theory (DFT). The theoretical features discovered through density functional theory (DFT) simulations such as the HOMO-LUMO value can be used

to identify the active sites. The aim of the theoretical study was to know the energy properties of the dye.

Keywords : B3LYP, HOMO level, LUMO level, DFT, eosin Y dye .

1- Introduction

1-1 Pollution

One of the biggest problems facing the world today is environmental degradation. Hazardous materials decompose more slowly in wild creatures. These days, we can quickly break down or accumulate dangerous materials from environments by combining traditional techniques with sophisticated molecular biology capabilities. By altering microorganisms, we can increase crop yields and cultivate plants by giving them the capacity to detect and break down dangerous compounds from contaminated areas. In order to enhance environmental conditions, this chapter highlights the use of both traditional and cutting-edge molecular biology techniques to remove and detoxify contaminants from soil and water.[1]

The release of pollutants into the Environment that results in negative changes is known as environmental pollution. Both chemicals and energy, such as heat, light, or noise, can be considered forms of pollution. Both naturally occurring contaminants and substances or energies from outside sources can be considered pollutants. Source pollution and non-source pollution are two common classifications for pollution. The phrase "pollution control" refers to environmental management. Controlling emissions and effluents into the air, water, or soil is what it means. Waste from mining, manufacturing, transportation, heating, overconsumption, and other human activities will deteriorate the environment if pollution is not controlled. Waste reduction and pollution prevention are preferred over pollution control in the hierarchy of controls.[2]

1-2 Adsorption

Surface adsorption process means water pollution problem .material that may attract molecules, atoms, or ions from other substances, whether they be gaseous or liquid, is known as an adsorbent. The surface on which the adsorption occurs is known as the adsorbent surface [3]. Although adsorption is considered an old technology, its applications and uses are so vital that no industry today can function without it. It is used in the food, dairy and petroleum industries, as well as in dyes and other industries that are countless here.[4]

1-3 The Dyes

The two most significant colouring compounds, dyes and pigments, are used to add or modify colour. People depend on them in many different sectors, including plastic, food, cosmetics, pharmaceuticals, photography, paint, ink, and paper. Dyes are colored materials that selectively absorb light to produce color. They are liquid or dissolve when applied. Finely split organic or inorganic solids, pigments can be luminous, colorless, or colored. They are basically chemically unaffected by the media or carrier in which they are included and are typically insoluble in it. On the other hand, color is the outcome of the interaction between light and the substance and is mostly determined by the chemical and physical characteristics of the substance[5] A luminous xanthine dye called eosin attaches itself to salts that include acidic chemicals with a positive charge. Using this dye in conjunction with alum haematoxylin is the gold standard for revealing the general histological structure of tissues. The proper use of eosin's reddish-pink staining spectrum allows for the separation of various cell cytoplasms, connective tissue fibres, and matrices. Though several varieties of eosin stain are available, the most popular and adaptable is eosin Y, which dissolves in both alcohol and water. The presence of condensed red blood cells causes eosin to turn red, which is why it is also employed as a red dye in inks. However, molecules like eosin Y have a tendency to deteriorate over[illegible]oms separate from eosin Y.[6]

Figure 1hemical Structure of the eosinY dye.

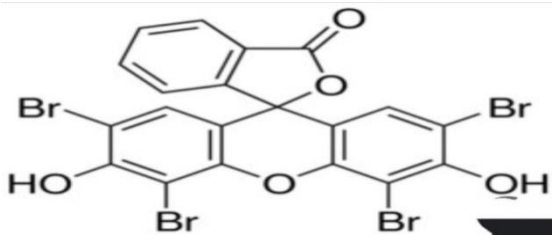

1.4 Adsorbents

Carbon Activation Indeed, when carbonized in an inert atmosphere, plants from all over the world can produce porous carbon. Activated carbon that can effectively carry out the necessary industrial applications is, nevertheless, rarely produced. Today's commercial activated carbon is the product of extensive and ongoing research and development aimed at enhancing its use. Activated carbon belongs to a family of carbons that includes nuclear graphite, carbon black, electrolytic graphite, carbon fibers and composites, and many more. Although their

carbonization and production procedures vary, they are all derived from original organic sources.[7]

1-5 Computational chemistry

Computational chemistry is a branch of chemistry that uses computer models to help solve chemical problems. In order to solve theoretical chemistry problems as quickly and cheaply as possible, and to know the energetic properties of the dye in terms of active sites and their surface binding, this branch of theoretical chemistry seeks to develop effective mathematical approximations. It also develops algorithms and programs that calculate molecular properties such as total energy, dipole and quadrupole moments, vibrational frequencies, reactivity, spectral quantities, and collision cross sections with molecules of different atomic and subatomic projections. As a result, many approximation techniques have been developed that balance processing cost and accuracy. Today, computational chemistry can determine the properties of molecules with fewer than 10–40 electrons with high accuracy and reproducibility. Although approximation techniques such as density functional theory (DFT) are commonly used to study molecules with several tens of electrons, experts still disagree about how well these techniques can describe complex chemical reactions, such as those in biochemistry.[8]

2.Methodology

Material

Nutshells, citric acid, sodium hydroxide, and sodium nitrite were provided by CDH (India), whilst nitric acid and hydrogen chloride were supplied by Himedia (India).

2.1. Surface preparation of the absorbent material

Carbon charcoal is made from walnut shells by periodically washing them with distilled water, letting them dry at 100 °C for two hours, and then baking them in an oxygen-free oven at 500 °C for two hours. A 0.1 μm sieve is then used to

filter the finely ground charcoal. Following five rounds of cleaning with distilled water, it is then dried for two hours at 50 °C [9].

2.2. Methods for Making Standard Solutions and Curves for Calibration

Preparation of standard solutions and calibration curve The standard solution of eosin yellow dye was prepared at a concentration of (500 ppm) by dissolving (0.250 g) in (500 ml) of distilled water. Then different concentrations of eosin yellow dye were prepared from (5 to 50 ppm) and a spectrum of the dye was taken using an ultraviolet and visible spectrometer to obtain lambda max where the maximum absorption was exploited using distilled water as a raw sample. Then the absorbance of each of the ten samples was measured by an ultraviolet and visible spectrometer to determine the calibration curve. (For eosin yellow dye).

2.3 Effect of Contact Time

At 298 K, activat carbon and dye were utilized in the experiment. The eosin yellow concentration in the 20 ml samples was 50 ppm. The weight of the activated carbon was 0.2 g. Intervals of0.5,1,1.5,2,2.5,3, and 3.5 hours were used, The samples were then shaken in a water bath to remove the colour. After that, they went through a filter paper. Lastly, ultraviolet-visible spectroscopy was used to ascertain the absorbance of the filtered samples. (10)

2.4.The effect of surface weight on the adsorption capacity of eosin Y dye

Investigating the effect of surface weight on adsorption capacity, we found the ideal contact length for eosin yellow dye at a constant temperature (298 K) and different weights (0.05, 0.1, 0.15, 0.2, 0.25, 0.3, 0.4, 0.5, 1) g and volume (20 ml). The samples were incubated in a shaking water bath with eosin yellow dye for 120 minutes, and then filtered through filter paper. The absorbance was measured using a UV-visible spectrophotometer (11).

2.5. Effect (pH)

The pH scale was used to evaluate the pH function in this research by taking six distinct concentrations of the dye (eosin yellow) at the highest concentration (2, 4, 6, 8, 10). Then each of these samples was given a constant surface weight, and The absorbance was measured using the UV-Vis spectrophotometer(12).

2.6 Effect of Zero Point

Twenty millilitres of eosin yellow dye, with a concentration of fifty parts per million, was divided into ten equal portions for this investigation. Afterwards, 0.3 g of activated charcoal, a constant surface weight, and 40 ml of sodium nitrate solution were added to each sample. The surface charge on which the adsorption process takes place was determined by leaving the mixture for 24 hours. Then, we calculated the surface charge by combining the results of the absorbance measurement with the beginning and finishing pH values(13).

ΔpH=pHf -pHi ……(1)

pHf= After Adsorption, pHi= before adsorption

2.7 Adsorption Isothermal

A range of quantities of eosin yellow dye, from 5 to 50 ppm, was used to create 10 samples. To a stationary surface, twenty millilitres of each concentration was applied. We filtered the samples using filter paper after subjecting them to a shaking water bath for 120 minutes. Next, UV-visible spectroscopy was used to quantify the absorbance.The samples were deposited into a shaking water bath, and after a specific period of time (for eosin yellow dye for 120 min), the samples were filtered with filter paper and the absorbance was measured in the UV spectrometer at the maximum corresponding to each of the two dyes, and the concentration after absorption (Ce) was detected through the calibration curve with the following equation (14).

qe = (o−$c\ e$) $V\ s\ o\ l$ .....(2)

m :where qe: the amount of absorbent (mg/g)

c o: the initial concentration of the dye (mg/L)

$c\ e$: the concentration at equilibrium of the dye (mg/L)

$c\ e$: the total volume of the absorbent, m : the weight of the absorbent (g)

3-Computational methods

We utilized Gauss View 06 to construct the eosinophilic yellow structure in the basis set 6-311G [15], where the geometry optimization structure was created, and Gaussian 09 to compute it using DFT/B3LYP. Additionally, we computed the energy difference between the orbitals, the transition energy between the least

occupied orbital (LUMO) and the highest occupied orbital (HOMO), and the total energy of the dye [16]. The electronegativity (χ) is the definition of the chemical potential (μ) in theoretical chemistry. [17] In this manner:

$\chi=1/2$ (E Lumo+E Homo) ……3

$\mu=-\chi=1/2$ (E Lumo+E Homo)…….. 4

The following is a quantitative description of the N-electron device's hardness (η) with total energy E [19].

$\eta=1/2$ (E Lumo-E Homo)……5

The universal electron affinity index (ω)[18] from which it is transferred as follows:

$\omega=-\mu 2/(2\ \eta)$ …… 6

where IP and EA stand for the chemical system's starting potentials for vertical ionization and electron affinity, respectively. The aforementioned parameters can be expressed as an extra approximation using Koopman's theorem. [19].

I = - E Homo …….. 7

A= - E Lumo ……... 8

Where the lowest energy unoccupied molecular orbital is known as ELUMO and the highest energy occupied molecular orbital is known as EHOMO. Furthermore, the UV-visible spectrum was calculated to determine the maximum wavelength of the eosin yellow pigment compound, and the infrared spectrum was used to diagnose the condition.

4-Result and Discussion

4.1 Calibration curve of eosin yellow dyes

It was determined that the dye had a maximum absorption wavelength of (512 eosin yellow) after measurements were taken. as shown in Figure 2). Meanwhile, the dual-spectrum UV-Vis spectroscopy was used to generate the calibration curve of the dye, with the dye λmax as shown in Figure (2).

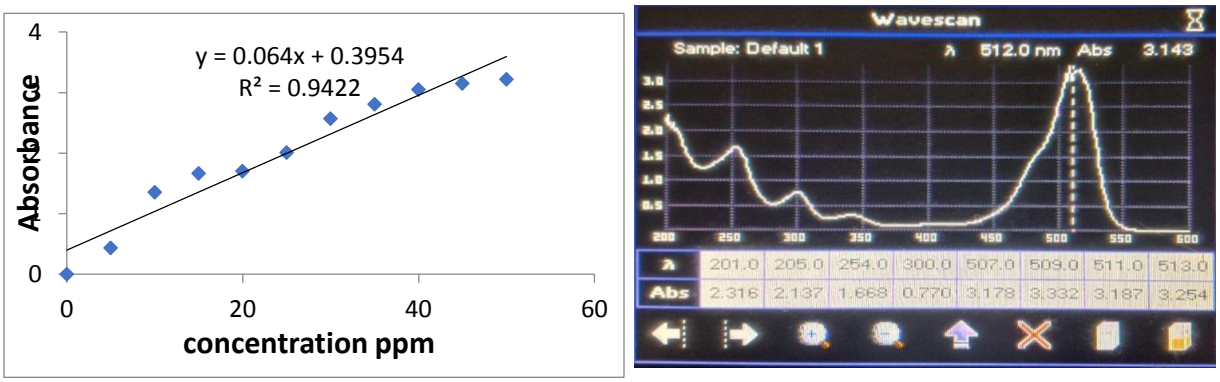

Figure (2) A-Calibration curve of eosinY , B- UV-visible spectra of eosin yellow dyes in distil water pH (6)

4.2 The contact time effect

This study was conducted to determine the ideal contact time between the dye and the activated surface made of walnut shells. The results based on the calculations indicated that the ideal contact time among the yellow eosin and the surface was 120 minutes,The high absorption quantity (Qe) is explained by the fact that the maximum dye absorption will take place there. The maximum amount of dye absorption will take place on the surface's active spots since they are empty. Following that, the colonization of these sites results in a decline in absorption capacity; that is, it eventually achieves a saturation condition with poor absorption. The absorption capacity rises and the activated surface's active sites are occupied at a particular contact period with this dye. Figure (3) depicts this effect in [20]

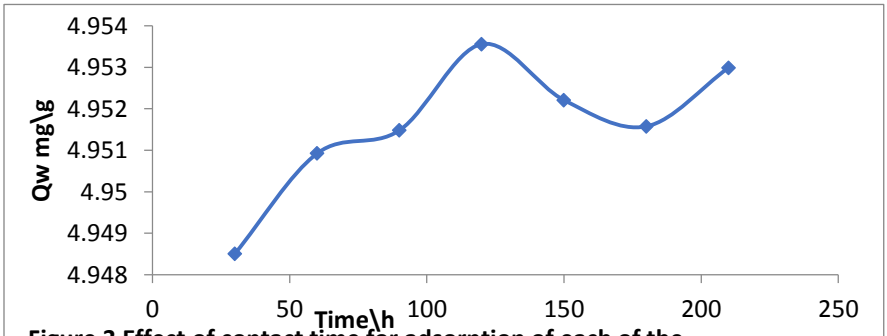

Figure 3 Effect of contact time for adsorption of each of the dye on the surface of activated carbon derived from walnut shells at pH = 6 and temperature 298 K

4.3 The Influence of Surface Weight on Dye Adsorption

The impact of the activated surface's weight, a crucial component in figuring out the dyes' ability to adsorb from their aqueous solutions, was investigated. As seen in Figure (4), the results indicated that the ideal weight for each of the yellow eosin dyes was 0.4 g.Because there were active sites, or surface area, available, the amount of adsorption on the activated carbon's surface was initially high when comparing the results. Following then, the amount of adsorption started to progressively decrease as the surface weight increased. On the one hand, this drop

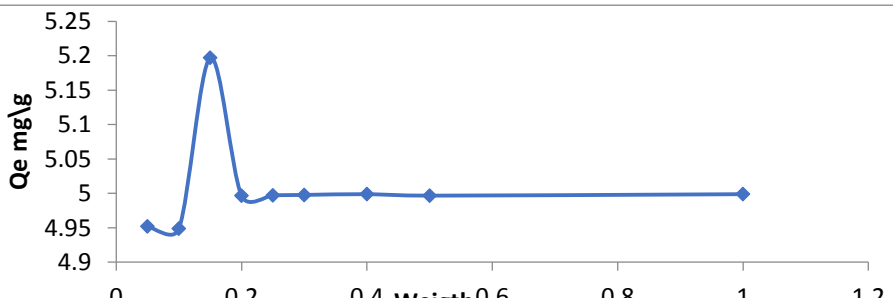

Figure 4 Effect of surface weight for adsorption of each of the dyes on the surface of activated carbon derived from walnut shells at pH = 6 and temperature 298 K

is ascribed to the accumulation of the adsorbed material (the dye) in the aqueous phase.

4.4 Temperature Effect.

Temperature significantly influences the practical applications of activated carbon and is crucial in adsorption studies to assess its impact on the efficacy of the adsorbent. The influence of temperature on the adsorption of eosin yellow dye onto walnut shell-derived charcoal was examined within the temperature range of 298 to 328 K, as seen in the figure below for each dye [21]. Experiments were performed at various temperatures. The results, as shown in Figure (5). show that the adsorption amount of eosin yellow dye on the surface of charcoal made from walnut shells decrease when the temperature rises to 298 and 328 K.

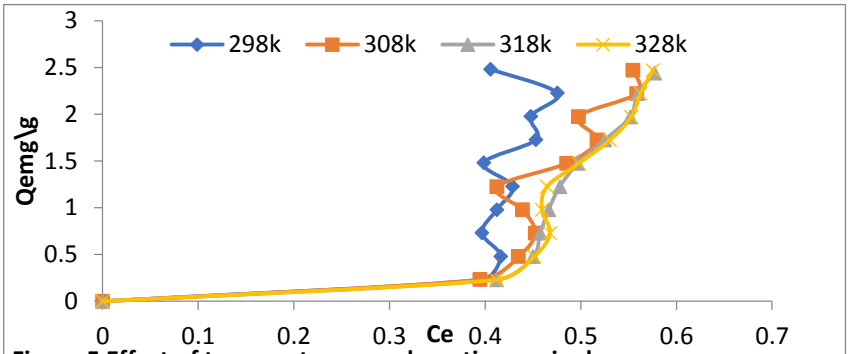

Figure 5 Effect of temperature on adsorption eosin dye on the surface of activated carbon derived from walnut shells at pH = 6 and temperature 298 k

4.5. Absorption Thermodynamics

equations on the following were used to assess the thermodynamic behavior of eosin yellow adsorption on activated charcoal, as stated in figure (6). [22]

$\Delta G = \Delta H - T\Delta S$ …….. (9)

$\ln K_C = -\Delta H/RT + \Delta S/R$ ……(10)

Enthalpy and entropy are derived by graphing Ln Xeq vs 1/T, where ΔH denotes enthalpy, ΔS signifies entropy, and ΔG indicates the change in free energy..

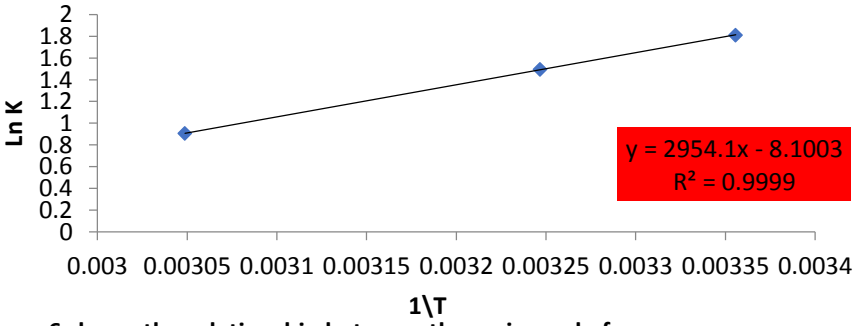

Figure 6 shows the relationship between the reciprocal of temperature and the equilibrium constant for the adsorption of dyes on the surface of activated carbon derived from walnut .shells at pH values of 298, 308, 318, 328 K and pH values of 6

4.6 Investigation of Adsorption Isotherm Models

Various forms of sorption isotherms are available, with the most often utilised being the Freundlich, Langmuir, Temkin, and Harkins-Jura isotherms. Any

of these can be utilised to optimally align with the data, depending on the characteristics of the provided data. Sorption isotherms are frequently utilised to graphically represent the relationship between the quantity of adsorbate retained by the adsorbent and the concentration of adsorbate on the adsorbent surface. Based on criteria, there are various kinds of isotherms [23].

4.6.1. Langmuir models

According to the isothermal Langmuir model, adsorption takes place on the absorbing materials' homogenous surfaces; in other words, it is single-layer adsorption. Sequential experiments were carried out using varying beginning concentrations of the dyes (eosin yellow) at varying temperatures (298 to 328 K) [24]. Figure 11 below illustrates these findings.

Ce/Qe= 1\Km.qm +Ce/qm ……..(11)

Where Ce (mg/L) is the equilibrium concentration, qe (mg/g) is the mass of eosin yellow adsorbed at equilibrium, qm (mg/g) is a concentration parameter related to the adsorption capacity of the monolayer of the adsorbent, and KL (L/mg) is the Langmuir constant related to the adsorption efficiency of the solute. Figure 1 shows a straight-line plot of Ce/qe versus Ce with a slope of Ce/qe and an intercept of (1/qm)(1/KL) (25). The parameters KL, qm, and the linear correlation coefficient R^2 are presented in Table 1.

Dyes	Qm	Kl	R^2
Eosin yellow	-0.2487	-1.8988	0.2589

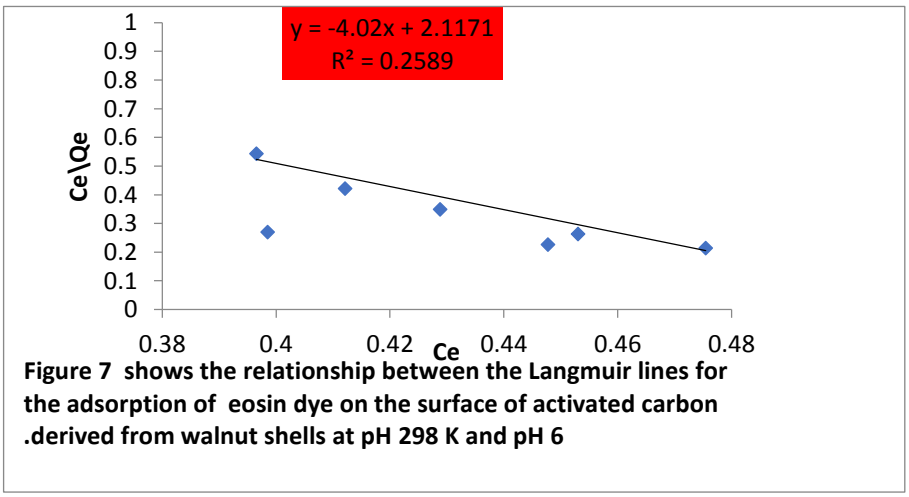

Figure 7 shows the relationship between the Langmuir lines for the adsorption of eosin dye on the surface of activated carbon .derived from walnut shells at pH 298 K and pH 6

4.6.2 Isotherm Freundlich.

Adsorption takes place on surfaces that are diverse and multilayered, as seen in Figure (8). Both Rose Bengal and Nile blue dyes were applied to the surface of walnut shell-derived charcoal between 298 and 328 K using the Freundlich adsorption equation. The calculated Freundlich constants are denoted by (n), indicating the degree of adsorption and the curvature of the saturation curve, and (Kf), which represents the adsorption capacity of the surface based on the slope and intercept. The constants are displayed in Table (2) when logQe is graphed against logCe utilising the equation. [26]

$$\text{Log Qe} = \text{Log Kf} + 1/n \text{ Log Ce} \qquad \text{…….(12)}$$

Where Kf and n are the system's Freundlich Constants property.

Dyes	N	Kf	R^2
Eosin yellow	0.2385	0.00177	0.2377

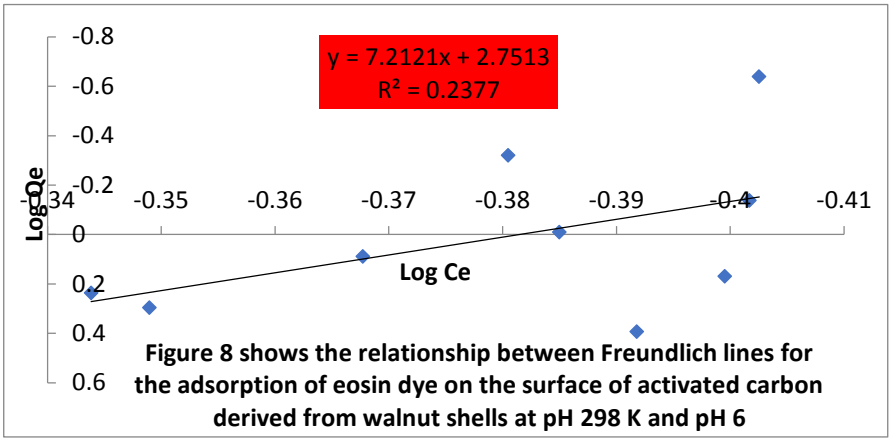

Figure 8 shows the relationship between Freundlich lines for the adsorption of eosin dye on the surface of activated carbon derived from walnut shells at pH 298 K and pH 6

4.6.3 Elovich Isotherm:

Elovich's model is expressed by an equation based on kinetic data, suggesting that the number of adsorption sites increases exponentially with adsorption. This indicates that adsorption takes place in several levels, and the relationship is expressed in the following equation [27]. The results are shown in Figure (9).

Ln qe/Ce=lnK.qm-1/ (qm. Qe) …….(13)

Dyes	Qm	K	R^2
Eosin yellow	0.09356	1.09808	0.2534

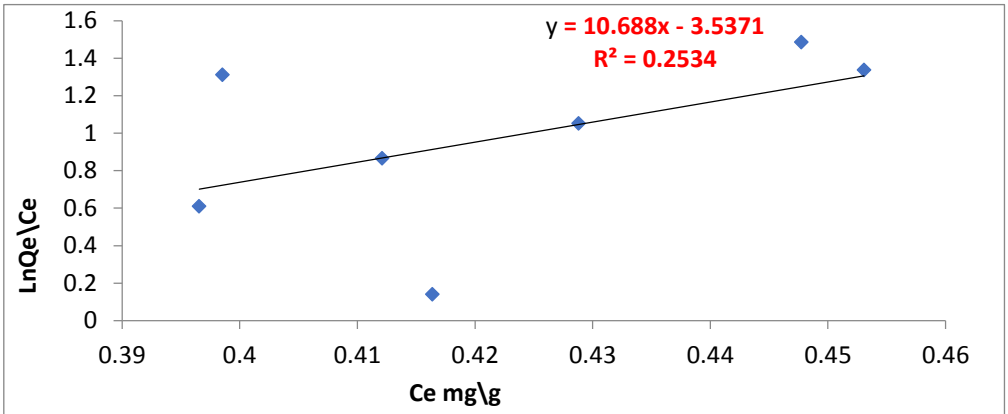

Figure 9 shows the relationship between the Elovish lines for the adsorption of eosin dye on the surface of activated carbon derived from walnut shells at pH 298 K and pH 6

4.6.4 Harkin -Jura Adsorption Isotherm:

The use of the Harkin equation reveals an extra parameter in the analysis of the isothermal properties of the adsorption process; the result is displayed in figure (10),

Where 1/qe2=B/A-1/A log Ce …..(14)

Where Ce stands for equilibrium concentration and qe for equilibrium adsorption. The Harkins-Jura isotherm parameter is A, while the isotherm constant is B. In this isotherm, multilayer adsorption is thought to take place in a heterogeneous pore distribution [28].

Dyes	A	B	R^2
Eosin yellow	-0.00904	0.35089	0.1608

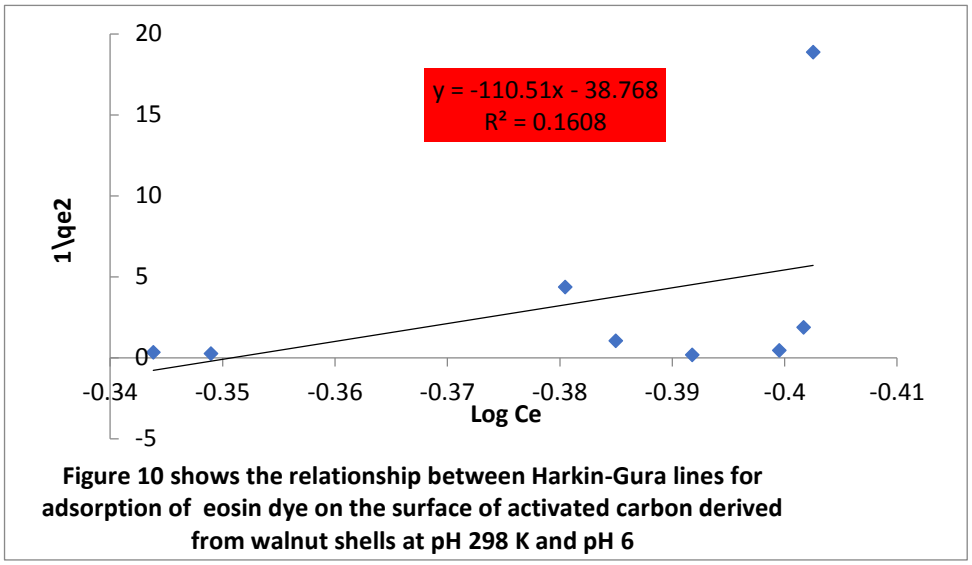

Figure 10 shows the relationship between Harkin-Gura lines for adsorption of eosin dye on the surface of activated carbon derived from walnut shells at pH 298 K and pH 6

4.6.5 Isotherm of Temkin

Furthermore, the Temkin parameter employs the subsequent equation[29] to denote the isothermal work of the adsorption process:

$$Qe = B \ln A + B \ln Ce \quad \text{.....(15)}$$

The Temkin constants A and B can be determined through a plot of Qe against ln Ce. The parameters, A and B, together with the correlation coefficient.

Figure (11), which displays the investigation's findings, shows that the adsorption process primarily follows the physical type

Dyes	B	KT	R^2
Eosin yellow	0.079	1.0823	0.6706

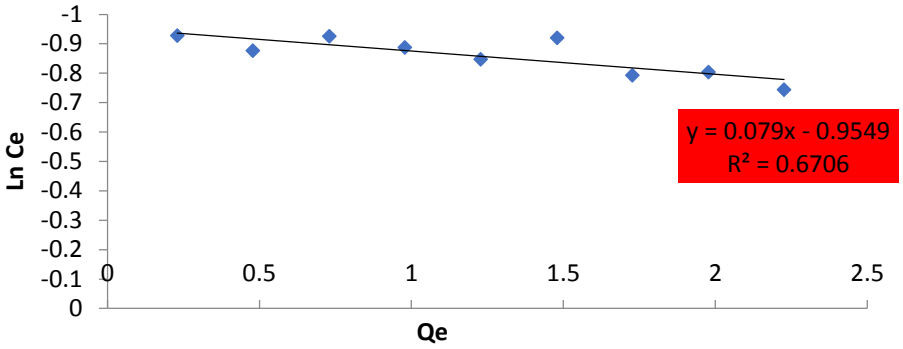

Figure 11 represents the relationship between the Temkin lines for the adsorption of eosin dye on the surface of activated carbon derived from walnut shells at pH 298 K and pH 6

4.6.6 Dubinin Isotherm:

Through the Dubinin-Radushkevich equation. The adsorption process on an inhomogeneous surface is often explained by a Gaussian energy distribution. [30].The result is shown in Fig. (12).

$$\text{Ln } Qe = \ln Qm - B\varepsilon 2 \quad \ldots\ldots(16)$$

$$\varepsilon = R\ T \ln(1+1/Ce) \quad \ldots\ldots\ldots(17)$$

Dyes	Qm	B	R^2
Eosin yellow	3.65419	-6E-07	0.1615

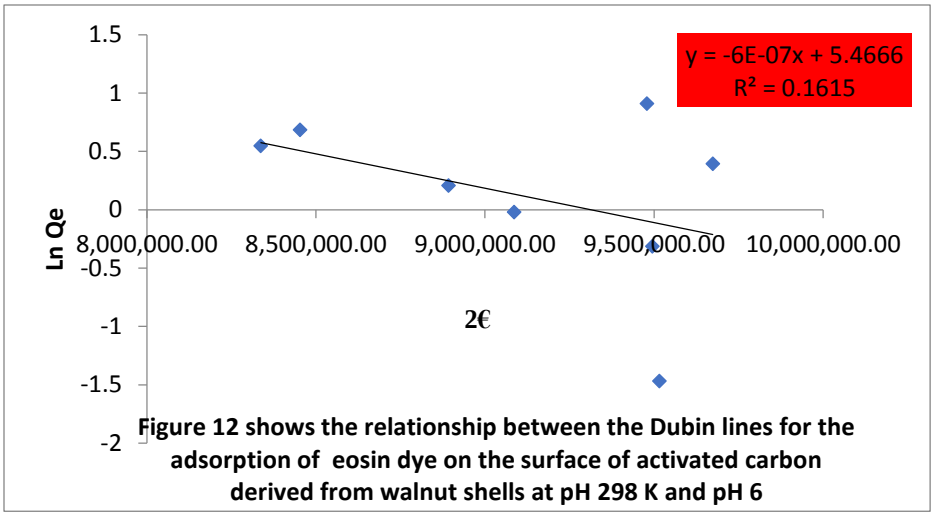

Figure 12 shows the relationship between the Dubin lines for the adsorption of eosin dye on the surface of activated carbon derived from walnut shells at pH 298 K and pH 6

5- Geometry optimization of the eosin yellow pigment

The idealized structure of the eosin yellow pigment, shown in Figure 13, DFT/B3LYP/6-311G, includes all of the pertinent findings from the current study

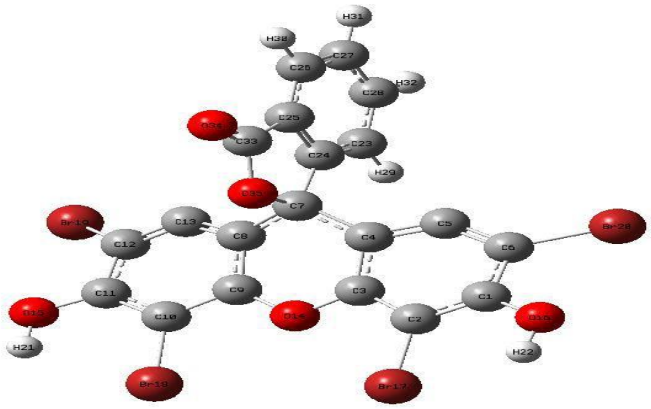

. Fig.13 Geometry optimized eosin yellow pigment by DFT/ B3LYP basis set 6-311G .

Properties of eosin Y

Molecular Electrostatic Potential

By drawing the molecules' peripheral surface ، we can predict and validate chemically active sites with high electronegativity and a center of positive charge

by examining the molecule's electrostatic potential, which provides a clear picture of the electronic density distribution of molecular systems [31].

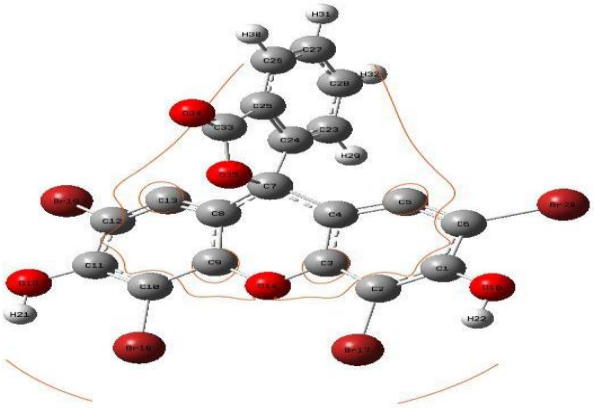

. Fig.14 ESP eosin yellow pigment by DFT/ B3LYP basis set 6-311G

Energy levels

Density Functional Theory (DFT) with the B3LYP/6-311G basis set was employed to compute the energies of the forward molecular orbitals of eosin yellow dye, specifically the highest occupied molecular orbital (EHOMO), the lowest unoccupied molecular orbital (ELUMO), and the energy gap (Egap). The ELUMO energy pertains to the capacity of molecules to accept electrons, whereas the energy associated with the electron-donating ability of EHOMO is typically linked to molecules themselves. [32]. High LUMO and EHOMO values suggest a significant propensity for electron acceptance and a strong capacity for electron donation, characterised by low energy in empty molecular orbitals suitable for interaction with acceptor molecules. Table 1 and Figure 5 present the results regarding the energy disparity between the HOMO and LUMO energy levels of eosin yellow dye [33]. Low energy gap values result in low electronic stability and high reactivity. Low values are advantageous as they suggest a facilitated extraction of an electron from the HOMO orbital to the LUMO orbital.

Table 1 . Levels of energy in eosin Y DFT/6-311G at levels of theory.

Functions	E_{LUMO}	E_{HOMO}	ΔE gap
Eosin Y	-0.14268	- 0.27937	0.13669

Fig.15

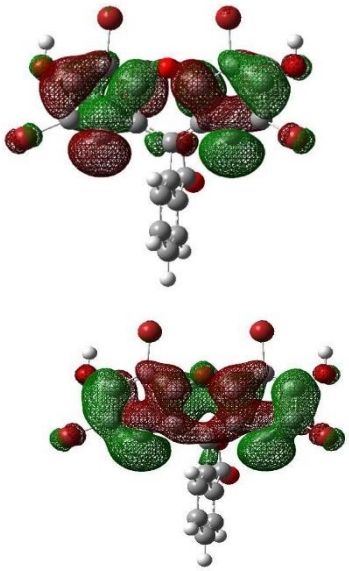

EHOMO=-0.27937

Egap=0.13669

ELUMO=-0.14268

The DFT/B3LYP basis set 6-311G provides the energy of the LUMO and HOMO molecular orbitals of Eosin yellow

Spectroscopy properties

1-UV-Visible spectrophotometer

Fig.16 This helps us explain why the resulting chemical has color since the visible range, which spans from 450 to 600 nm, is covered by the absorption peak seen in

the image, which was detected by UV-Vis spectroscopy at a maximum wavelength of 512 nm.

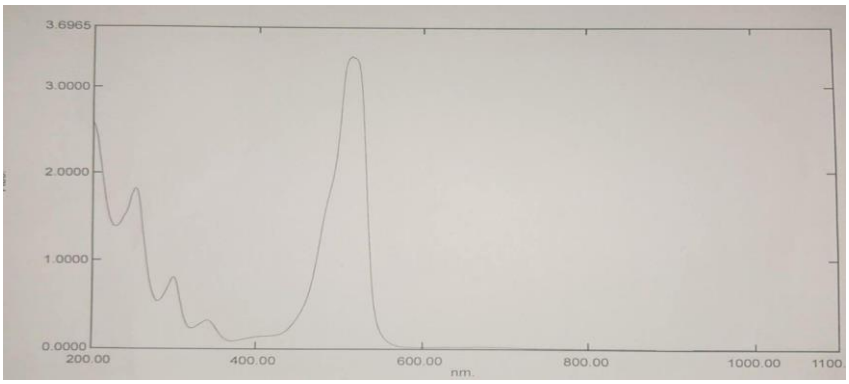

Fig. 16. UV- visible spectroscopy of eosin Y by DFT/ B3LYP basis set 6-311G .

2-Infrared spectroscopy

We looked at the ground state harmonic vibration frequencies of the 6-311G base groups in Fig. 17, B3LYP, and eosin yellow dye. Asymmetric and symmetric stretching anomalies were the two categories of stretching anomalies. The symmetric stretching happened at the same time as the atoms' vibration, whereas the asymmetric stretching happened at different times during the bonds' vibration.Multiple aliphatic (C-H) stretching vibrations are found around 1500 cm-1. [34]. C=C, appears at 1800 cm-1 and C-O appears at 1200 cm-1. C-Br appears at 600 cm-1. Vibrational decomposition calculations of eosin yellow dye were performed. [35].

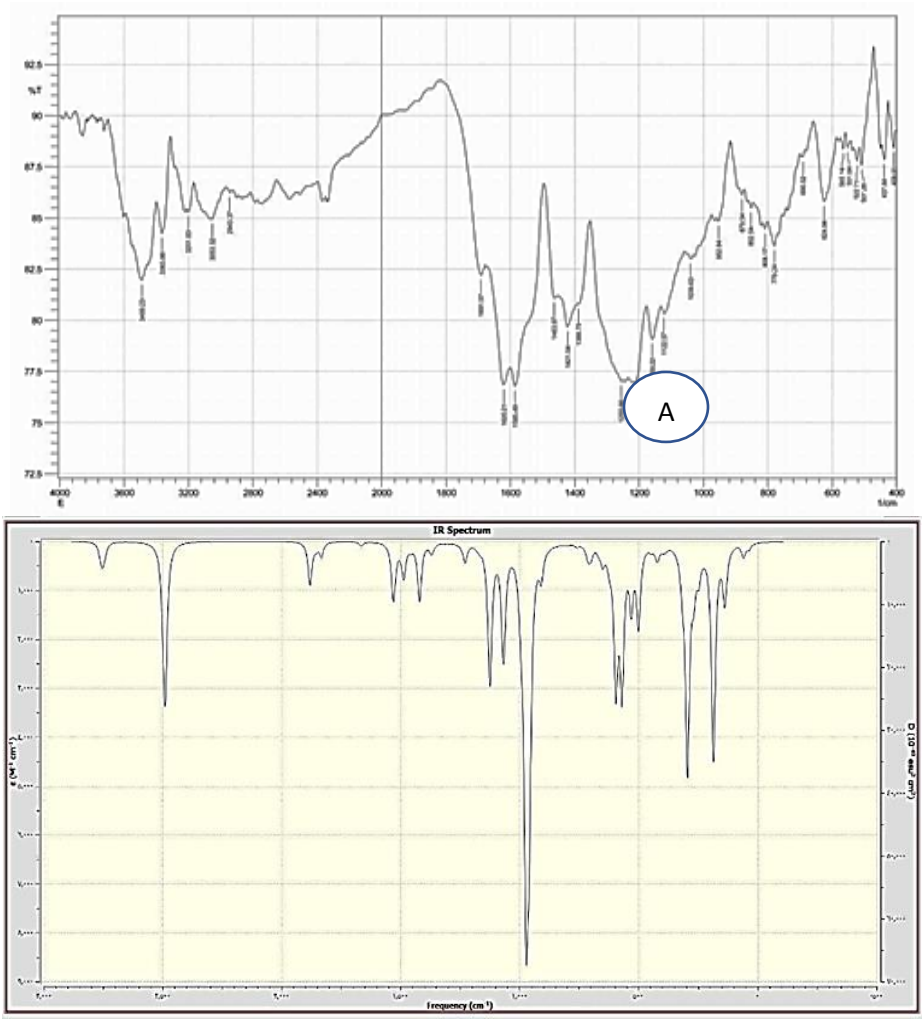

Fig. 17. Eosin Y A- infrared the experimental spectrum B- theoretical spectrum using DFT/B3LYP basis set 6-113G.

References

[1] Vimal Chandra Pandey, Vijay Singh, in Vegetation Management in Contaminated Sites ,2019

[2] Riffat, Saffa, et al. "Environmental Pollution and Control." Environmental Pollution and Control (2016): 314.

[3] Zhang, Hongguang, Ian M. Ritchie, and Steve R. La Brooy. "The adsorption of gold thiourea complex onto activated carbon." Hydrometallurgy 72.3-4 (2004): 291-301.

[4] Tsareva, A. A., et al. "Kinetic Calculation of Sorption of Ethyl Alcohol on Carbon Materials." Russian Journal of Physical Chemistry A (2024): 1-10.

[5] John D. Bancroft, Christopher Layton, in Bancroft's Theory and Practice of Textile Techniques (8th Edition), 2019

[6] Gürses, Ahmet, et al. "Dyes and pigments: their structure and properties." Dyes and pigments (2016): 13-29.

[7] Marsh, Harry, and Francisco Rodríguez Reinoso. Activated carbon. Elsevier, 2006.

8- سيف الدين موفق عبد الهادي. "اتجاه تقنية النمذجة (الإمكانات البينية) لدراسة الأسطح and سماء البياتي, مجلة سامراء للعلوم الصرفة والتطبيقية 2.3 (2020): 62-73." Array: مراجعة المعدنية:.

[9]Hasana, N. H., R. Wahi, and Y. Yusof. "Ethanol, Methanol, and Magnesium-Treated Palm Kernel Shell Biochar for Methylene Blue Removal: Adsorption Isotherms." Int J Cur Res Rev| Vol 13.04 (2021): 2.

[10]Imteaz, Monzur Alam, Maryam Bayatvarkeshi, and Amimul Ahsan. "Modelling Metribuzin removal efficiency through adsorption using activated carbon of olive-waste cake." Water, Air, & Soil Pollution 233.4 (2022): 115.

[11]Show, Sumona, Bisheswar Karmakar, and Gopinath Halder. "Sorptive uptake of anti-inflammatory drug ibuprofen by waste biomass–derived biochar: experimental and statistical analysis." Biomass Conversion and Biorefinery (2020): 1-19.

[12]Aldawsari, Abdullah Mohammed, et al. "Adsorptive performance of aminoterephthalic acid modified oxidized activated carbon for malachite green dye: mechanism, kinetic and thermodynamic studies." Separation Science and Technology 56.5 (2021): 835-846.

[13] Parimelazhagan, Vairavel, et al. "Rapid removal of toxic Remazol brilliant blue-R dye from aqueous solutions using Juglans nigra shell biomass activated carbon as potential adsorbent: Optimization, isotherm, kinetic, and thermodynamic investigation." International Journal of Molecular Sciences 23.20 (2022): 12484.

[14] Saraswati, N. L. P. A., and I. D. K. Sastrawidana. "Absorption of Remazol Red dye from textile waste using activated carbon from coconut shell." IOP Conference Series: Materials Science and Engineering. Vol. 1115. No. 1. IOP Publishing, 2021.

[15] Mubarik, Adeel, et al. "Computational study of structural, molecular orbitals, optical and thermodynamic parameters of thiophene sulfonamide derivatives." Crystals 11.2 (2021): 211.

[16] Veclani, Daniele, et al. "Intercalation ability of novel monofunctional platinum anticancer drugs: a key step in their biological action." Journal of Chemical Information and Modeling 61.9 (2021): 4391-4399.

[17] Tandon, Hiteshi, Tanmoy Chakraborty, and Vandana Suhag. "A fundamental approach to compute atomic electrophilicity index." Journal of Mathematical Chemistry 58 (2020): 2188-2196.

[18] Midoune, Assia, and Abdelatif Messaoudi. "DFT/TD-DFT computational study of the tetrathiafulvalene-1, 3-benzothiazole molecule to highlight its structural, electronic, vibrational and non-linear optical properties." Comptes Rendus. Chimie 23.2 (2020): 143-158.

[19] Pan, Sudip, Miquel Solà, and Pratim K. Chattaraj. "On the validity of the maximum hardness principle and the minimum electrophilicity principle during chemical reactions." The Journal of Physical Chemistry A 117.8 (2013): 1843-1852.

[20] Turner, James Edward, V. E. Anderson, and Kenneth Fox. "Ground-state energy eigenvalues and eigenfunctions for an electron in an electric-dipole field." Physical Review 174.1 (1968): 81.

[21] Altıntıg, Esra, et al. "Effective removal of methylene blue from aqueous solutions using magnetic loaded activated carbon as novel adsorbent." Chemical Engineering Research and Design 122 (2017): 151-163 .

[22] Kausar, Abida, et al. "Chitosan-cellulose composite for the adsorptive removal of anionic dyes: Experimental and theoretically approach." Journal of Molecular Liquids 391 (2023): 123347.

[23] Theivarasu, C., and S. Mylsamy. "Removal of Malachite Green from Aqueous Solution by Activated Carbon Developed from Cocoa (Theobroma Cacao) Shell-A Kinetic and Equilibrium Studies." Journal of Chemistry 8 (2011): S363-S371.

[24] Algidsawi, Alaa Jewad K. "A Study of ability of adsorption of some dyes on activated carbon from date's stones." Australian Journal of Basic and Applied Sciences 5.11 (2011): 1397-1403.

[25]Arslan, Yasin, et al. "Determination of adsorption characteristics of orange peel activated with potassium carbonate for chromium (III) removal." Journal of the Turkish Chemical Society Section A: Chemistry 4.1 (2017): 51-64.

[26]Kallel, Fatma, et al. "Sorption and desorption characteristics for the removal of a toxic dye, methylene blue from aqueous solution by a low cost agricultural by-product." Journal of Molecular Liquids 219 (2016): 279-288.

[27]Ghorbanian, Sohrab A., Nafiseh Bagheri, and Amir Khakpay. "Investigation of adsorption isotherms of benzoic acid on activated carbon." Proceedings of the 1st National Conference on Industrial Water and Wastewater Treatment, Bandar Mahshahr, Iran. Vol. 29. 2012.

[28] Ramutshatsha-Makhwedzha, Denga, et al. "Activated carbon derived from waste orange and lemon peels for the adsorption of methyl orange and methylene blue dyes from wastewater." Heliyon 8.8 (2022).

[29]Chandana, L., et al. "Low-cost adsorbent derived from the coconut shell for the removal of hexavalent chromium from aqueous medium." Materials Today: Proceedings 26 (2020): 44-51.

[30]Dulla, John Babu, et al. "Biosorption of copper (II) onto spent biomass of Gelidiella acerosa (brown marine algae): optimization and kinetic studies." Applied Water Science 10.2 (2020): 56.

[31]Gordon, Mark S., et al. "Self-consistent molecular-orbital methods. 22. Small split-valence basis sets for second-row elements." Journal of the American Chemical Society 104.10 (1982): 2797-2803.

[32] Shi, Gai, et al. "Kinetics study on the reactions of dimethyl ether with triplet oxygen and hydrogen atoms." Chemical Physics Letters 779 (2021): 138855.

[33] Sahadevan, Madhavi, Karunagaran Subramanian, and Mullainathan Sundaram. "Quantum mechanical approaches and molecular docking studies of platinum based anticancer drugs Satraplatin and picoplatin structures." Biochemical and Biophysical Research Communications 739 (2024): 150969.

[34] Almutairi, Maha S., et al. "FT-IR and FT-Raman spectroscopic signatures, vibrational assignments, NBO, NLO analysis and molecular docking study of 2-{[5-(adamantan-1-yl)-4-methyl-4H-1, 2, 4-triazol-3-yl] sulfanyl}-N, N-dimethylethanamine." Spectrochimica Acta Part A: Molecular and Biomolecular Spectroscopy 140 (2015): 1-14..

[35] Palafox, M. A., and V. K. Rastogi. "The biomolecule of 5-chlorocytosine: Geometry of the six main tautomers in the isolated state by DFT calculations, and interpretation of the FT-IR and FT-Raman spectra in the solid state." Asian Chem Letts 19 (2015): 1-25.